ORIGINAL ARTICLE

Clinical, radiological, and anatomopathological characteristics of patients with atypical teratoid rhabdoid tumor at a national pediatric referral center in Lima, Peru

Alberto Ramírez Espinoza[1], Edwin Dominguez Crisanto[1], Carla Cruzado-Villanueva[2]

[1] Specialized Comprehensive Neurosurgery Care Subunit, Instituto Nacional de Salud del Niño San Borja, Lima 15037, Peru.
[2] Diagnostic Support Subunit, Pathology Service, Instituto Nacional de Salud del Niño San Borja, Lima 15037, Peru.

ABSTRACT

Objective: To describe the clinical, radiological, and anatomopathological characteristics of patients diagnosed with atypical teratoid rhabdoid tumor (ATRT) treated at a national referral center in Lima, Peru.
Methods: Patients aged < 18 years diagnosed with ATRT and treated at the Instituto Nacional de Salud del Niño San Borja between 2017 and 2024 were included. Sociodemographic data, clinical manifestations, immunohistochemical findings, and computed tomography and magnetic resonance imaging findings at diagnosis were collected from medical records. Data analysis was performed using Microsoft Excel version 16.104.
Results: Fourteen patients were included, aged between 7 months and 12 years, with a predominance of males. The most frequent clinical manifestation was vomiting (85.7%), followed by hydrocephalus. The predominant tumor location was supratentorial (57.1%), followed by infratentorial and spinal locations. Imaging studies showed variable radiological presentations. Diagnosis was confirmed by immunohistochemistry in all cases, demonstrating loss of nuclear INI1 expression, and rhabdoid cells were identified in most cases (64.3%).
Conclusions: In our cohort, ATRTs showed variable clinical and radiological presentations. This study contributes to the characterization of this rare neoplasm in the national context.

Keywords: Teratoid Tumor; Central Nervous System Neoplasms; Pediatrics; Immunohistochemistry; Diagnostic Imaging (Source: MeSH)

Cite as:
Ramírez Espinoza A, Dominguez Crisanto E, Cruzado-Villanueva C. Clinical, radiological, and anatomopathological characteristics of patients with atypical teratoid rhabdoid tumor at a national pediatric referral center in Lima, Peru. Investig Innov Clin Quir Pediatr. 2026;4(1):36-46.
doi: 10.59594/iicqp.2026.v4n1.161

Corresponding author:
Alberto Ramírez Espinoza
Email: alberto386@hotmail.com

ORCID iDs
Alberto Ramírez Espinoza
https://orcid.org/0000-0003-3530-5704
Edwin Dominguez Crisanto
https://orcid.org/0009-0009-6973-433X
Carla Cruzado-Villanueva
https://orcid.org/0009-0001-3813-9345

Received : 12/15/2025
Accepted : 02/20/2026
Published : 04/15/2026

Características clínicas, radiológicas y anatomopatológicas de pacientes con tumor teratoide rabdoide atípico en un centro pediátrico de referencia nacional en Lima, Perú

RESUMEN

Objetivo: Describir las características clínicas, radiológicas y anatomopatológicas de pacientes diagnosticados con tumor teratoide rabdoide atípico (ATRT) atendidos en un centro de referencia nacional de Lima, Perú.
Métodos: Se incluyeron pacientes menores de 18 años con diagnóstico de ATRT, atendidos en el Instituto Nacional de Salud del Niño San Borja entre 2017 y 2024. Se recopilaron datos sociodemográficos, manifestaciones clínicas, hallazgos de inmunohistoquímica y hallazgos de la tomografía computarizada y resonancia magnética al diagnóstico, a partir de la historia clínica. El análisis de los datos se realizó utilizando el programa Microsoft Excel versión 16.104.
Resultados: Se incluyeron 14 pacientes, con edades entre 7 meses y 12 años, con predominio del sexo masculino. La manifestación clínica más frecuente fue el vómito (85,7 %), seguida de la hidrocefalia. La localización tumoral predominante fue la supratentorial (57,1 %), seguida de la infratentorial y la espinal.

Los estudios de imagen evidenciaron una presentación radiológica variable. El diagnóstico se confirmó mediante inmunohistoquímica en todos los casos, evidenciándose pérdida de la expresión nuclear de INI1, y en la mayoría se identificaron células rabdoides (64,3 %). **Conclusiones**: Los ATRT mostraron en nuestra cohorte una presentación clínica y radiológica variable. Este estudio contribuye a la caracterización de esta neoplasia poco frecuente en el contexto nacional.

Palabras clave: Tumor Teratoideo; Neoplasias del Sistema Nervioso Central; Pediatría; Inmunohistoquímica; Diagnóstico por Imagen (Fuente: DeCS)

INTRODUCTION

Atypical teratoid rhabdoid tumors (ATRTs) are highly aggressive pediatric brain tumors that usually occur at a very early age (0–3 years) and have a poor prognosis (1). They are the most common malignant central nervous system (CNS) tumors in children under 1 year of age and account for approximately 1–2% of all pediatric brain tumors (2). In this age group, ATRTs represent around 20% of embryonal CNS tumors and up to 40–50% of all malignant CNS neoplasms in the first year of life (3).

The genetic hallmark of these tumors is biallelic inactivation of the *SMARCB1* (*INI1*) gene and, less frequently, the *SMARCA4* (*BRG1*) gene. Up to 30% of cases are associated with constitutional heterozygous pathogenic variants in one of these genes, giving rise to rhabdoid tumor predisposition syndromes (4).

Histopathologically, ATRT is characterized by the presence of rhabdoid cells, with or without areas resembling a typical embryonal tumor, as well as epithelial and mesenchymal neoplastic tissue. The rhabdoid cell exhibits an eccentric round nucleus, abundant eosinophilic cytoplasm, and a prominent nucleolus, with frequent necrosis and high mitotic activity. Immunohistochemical analysis usually shows expression of vimentin and epithelial membrane antigen (EMA), along with other markers such as integrase interactor 1 (INI1), myogenic differentiation 1 (MyoD1), S-100 protein, smooth muscle actin (SMA), and glial fibrillary acidic protein (GFAP) (5). Although histopathological features may be suggestive, they are not sufficient on their own to establish the diagnosis of ATRT; this is confirmed by demonstrating loss of nuclear INI1 expression by immunohistochemistry, together with a complementary panel of markers (5).

The diagnosis of ATRT is established as part of an integrated evaluation according to the World Health Organization Classification of Tumors of the Central Nervous System, which combines histopathological, immunohistochemical, and, when available, molecular findings (6).

ATRTs have been described in various locations within the CNS, both supratentorial and infratentorial, and their distribution may vary according to age (7). In the infratentorial region, they mainly occur in the cerebellar hemisphere, the cerebellopontine angle, and the brainstem; in the supratentorial region, in the cerebral hemispheres. Spinal location is extremely rare (8).

On non-contrast computed tomography (CT), ATRTs usually appear as hyperdense lesions due to a high nucleus-to-cytoplasm ratio. On magnetic resonance imaging (MRI), they generally appear iso- or hypointense relative to gray matter on T1-weighted images, are heterogeneous with variable signal intensity on T2-weighted images, and show enhancement after contrast administration (9). Diffusion MRI plays an important role in the diagnosis of pediatric posterior fossa tumors, particularly medulloblastomas and ATRTs, because signal characteristics may reflect high cellularity and, therefore, tumor grade and aggressiveness (10).

Surgery is the main therapeutic option and consists of resection of the primary lesion, which can be classified into four groups according to the degree of tumor removal: gross total resection (no tumor), subtotal resection (90–99% of tumor removed), partial resection (50–89% of tumor removed), and suboptimal resection (<50% of tumor removed or biopsy only) (11). Surgical resection of ATRTs is often necessary due to intracranial hypertension, mass effect, hydrocephalus, and the need for diagnostic tissue (12).

Metastatic staging of ATRTs is performed using brain and spinal MRI, along with cerebrospinal fluid cytology, using the modified Chang system when information is available (13). Metastatic dissemination at initial presentation occurs in approximately 20–40% of cases and has been inconsistently associated with survival (3).

ATRTs are associated with limited overall survival, with few therapeutic advances over time. Several studies have shown that surgical resection is associated with improved survival outcomes (median overall survival of 50.3 months in patients undergoing surgery versus 28 months in those who did not) (14). On the other hand, supratentorial tumors have a more favorable prognosis (5-year overall survival of 51.95%) compared with tumors in other locations (15).

Given the rarity of ATRTs in the pediatric population, most available evidence comes from small series or studies conducted in high-income countries, with limited information from low- and middle-income countries, particularly in Latin America. In Peru, there are no published studies describing the clinical, immunohistochemical, and radiological characteristics of this entity, which limits understanding of its presentation in our setting and hinders comparison with international literature.

In this context, this study aimed to describe the clinical, radiological, and immunohistochemical characteristics of patients diagnosed with ATRT treated at a national pediatric referral center in Lima, Peru.

METHODS

Study type

This was an observational, descriptive, retrospective study.

Study population (inclusion and exclusion criteria)

The study population consisted of patients under 18 years of age diagnosed with ATRT, treated, admitted, hospitalized, and who underwent surgery at the Instituto Nacional de Salud del Niño San Borja between 2017 and 2024.

Patients with a confirmed diagnosis of ATRT, based on histopathological evaluation and complemented by immunohistochemistry of the tumor sample obtained during surgery, and with complete information on study variables recorded in the medical records were included. Patients who underwent a second surgery for residual or recurrent tumor with a different histopathological diagnosis were excluded.

Data collection, study variables, and statistical analysis

Information was collected from the review of medical records, as well as imaging, histopathology, and immunohistochemistry reports available in institutional records. Collected variables included age, sex, clinical manifestations, tumor location, CT and MRI findings, and histopathological and immunohistochemical results used for diagnostic confirmation. Data were recorded in a spreadsheet database (Microsoft Excel).

Tumor location was classified into three groups: supratentorial, infratentorial, and spinal.

Quantitative variables were summarized using means and standard deviations, as well as medians and interquartile ranges (Q3–Q1). Categorical variables were described using frequencies and percentages. Data processing was performed using Microsoft Excel version 16.104 (Microsoft Corporation, Redmond, WA, USA).

Ethical considerations

As this was a study based on retrospective data collection from medical records, imaging studies, and immunohistochemistry results, there was no direct patient contact. Confidentiality and anonymity of the collected information were ensured. Access to the database was restricted to the principal investigator, and data were coded for study use.

The study was approved by the Institutional Research Ethics Committee of the Instituto Nacional de Salud del Niño San Borja (Code PI-899).

RESULTS

Of the 14 cases, males predominated (64.3%). Age ranged from 7 to 144 months; the median was 43 months, with an interquartile range of 28.5 months, and the mean was 49 months with a standard deviation of 41.3 months.

Table 1 describes the clinical manifestations of the patients included in the study. The most frequent clinical manifestation was vomiting, which occurred in 12/14 patients (85.7%), followed by hydrocephalus in 10/14 patients (71.4%), of whom 7 were treated with ventriculoperitoneal shunt and 3 with external ventricular drainage. Headache was the third most common manifestation, occurring in 6/14 patients (42.9%). Other manifestations, such as tremor, increased head circumference, and sphincter dysfunction, were observed in only 1 of 14 patients (Table 1).

Thirteen of the 14 cases were intracranial (92.9%). Eight patients (57.1%) had tumors located in the supratentorial region (5 of them were ventricular). In 5 patients, the tumor was located in the infratentorial region, and there was only 1 case of spinal location in the lumbar region (Figure 1). In addition, one patient presented with leptomeningeal dissemination, and another had leptomeningeal dissemination with cerebellar and thalamic metastases.

Table 1. Clinical manifestations of the patients included in the study

Symptom	n	%
Vomiting	12	85.7
Hydrocephalus	10	71.4
Headache	6	42.9
Somnolence	5	35.7
Ataxia	5	35.7
Hemiparesis	3	21.4
Seizure	2	14.3
Decreased strength in lower limbs	2	14.3
Lower limb pain	2	14.3
Tremor	1	7.1
Increased head circumference	1	7.1
Sphincter dysfunction	1	7.1
Others	1	7.1

Surgical approaches were aimed at maximizing tumor resection; therefore, 13 of the 14 patients underwent craniotomy. Regarding the management of hydrocephalus, present in 10 patients, 7 were treated with ventriculoperitoneal shunt and 3 with external ventricular drainage (Table 2).

Of the 14 patients, 10 were evaluated with non-contrast brain CT, and 5 also underwent contrast-enhanced CT. CT findings are described in Table 3. In the non-contrast CT group, 6 lesions with a solid-cystic pattern were identified, 2 lesions with a solid isodense pattern, 1 lesion with a homogeneous solid pattern, and 1 lesion with a heterogeneous isodense pattern. In the contrast-enhanced CT group, 4 patients showed solid areas with heterogeneous enhancement, of whom 2 also had areas of necrosis. In this same group, one patient showed heterogeneous enhancement throughout the entire tumor.

Brain MRI was performed in 9 of the 14 patients, evaluating T1, T2, FLAIR, and diffusion sequences. MRI findings are detailed in Table 4. Of these 9 patients, 5 had supratentorial lesions (Figure 2), 3 had infratentorial lesions (Figure 3), and 1 had a lumbar lesion (Figure 4). On T1-weighted sequences, 5 lesions appeared isointense and 4 hypointense. On T2-weighted sequences, among the 8 patients in whom this finding was described, 6 lesions were isointense and 2 showed intermediate signal intensity. On diffusion sequences, 8 of the 9 patients showed diffusion restriction. After contrast administration in T1 sequences, among the 8 patients in whom this finding was described, 7 showed mild enhancement and 1 showed heterogeneous enhancement.

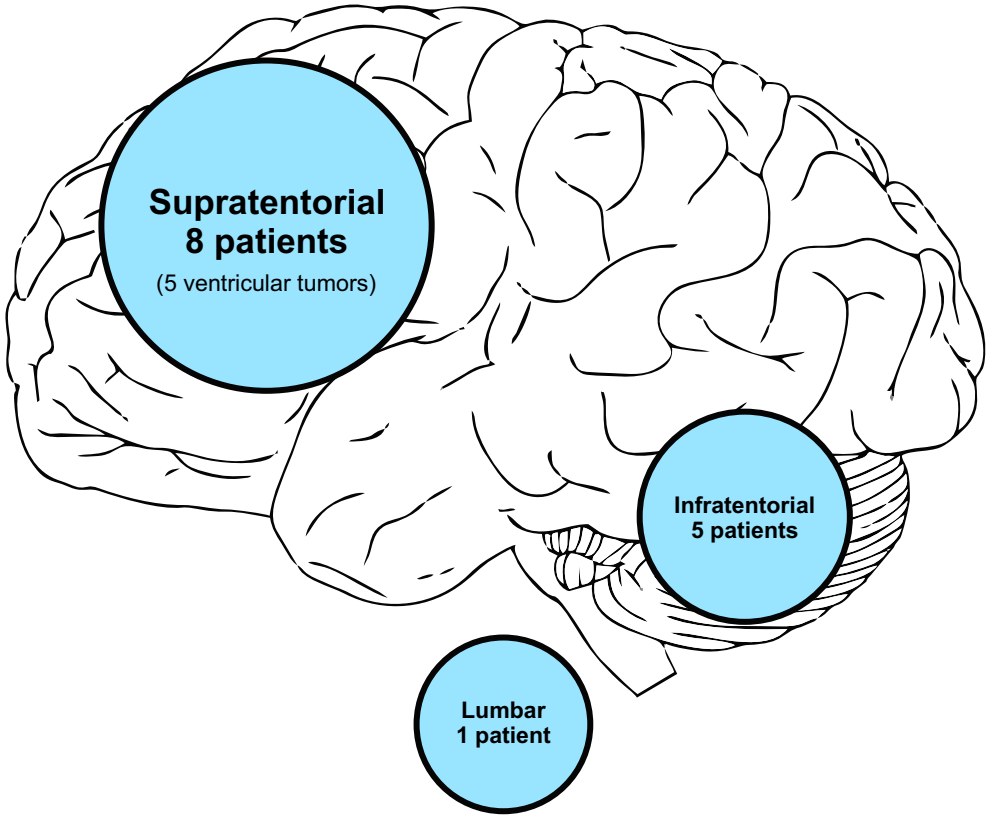

Figure 1. Distribution of tumors according to their location

Table 2. Surgical treatment according to tumor location in patients with ATRT

Case	Tumor location	Surgical approach to the tumor	Surgical management of hydrocephalus
1	Supratentorial ventricular	Right frontotemporal craniotomy	-
2	Infratentorial	Suboccipital craniotomy	VPS
3	Infratentorial	Left parieto-occipital parasagittal craniotomy + transtentorial approach	EVD
4	Supratentorial ventricular	Left frontal craniotomy	VPS
5	Supratentorial ventricular	Left frontal craniotomy	EVD
6	Supratentorial ventricular	Left frontal craniotomy + left transcortical transventricular approach	VPS
7	Infratentorial	Suboccipital craniotomy	VPS
8	Lumbar	Multiple lumbar laminectomies	-
9	Left frontotemporal supratentorial	Left frontoparietal craniotomy	-
10	Right frontoparietotemporal supratentorial	Right parietotemporal craniotomy	EVD
11	Infratentorial	Right suboccipital craniotomy	VPS
12	Supratentorial ventricular thalamic-mesencephalic	Right parietal craniotomy	VPS
13	Right frontoparietotemporal supratentorial	Right frontoparietal craniotomy	-
14	Infratentorial (right CPA)	Right retrosigmoid craniotomy	VPS

-: Patients without hydrocephalus. VPS: ventriculoperitoneal shunt; EVD: external ventricular drainage; CPA: cerebellopontine angle.

Table 3. CT findings of the analyzed cases

Case	Non-contrast	Contrast-enhanced
1	Heterogeneous solid-cystic	-
2	Solid-cystic, no calcifications	Solid areas show heterogeneous enhancement
3	Heterogeneous isodense with calcifications	Solid areas show heterogeneous enhancement with necrosis
4	Solid-cystic, no calcifications	-
8	Homogeneous solid isodense	Heterogeneous enhancement
10	Heterogeneous solid-cystic with calcifications	-
11	Heterogeneous solid-cystic, edema	-
12	Homogeneous solid with areas of necrosis	Solid areas show heterogeneous enhancement with necrosis
13	Homogeneous solid isodense	-
14	Solid-cystic, hemorrhagic content, surrounding vasogenic edema	Solid areas show heterogeneous enhancement

-: Contrast-enhanced CT was not performed.

Table 4. MRI findings of the analyzed cases

Caso	T1	T2	T2/FLAIR	Difusión	T1 contrastada	Compromiso leptomeníngeo
4	Isointense, solid-cystic	Heterogeneous isointense	-	Restricted	Mild enhancement	-
5	Isointense with hemorrhage	Heterogeneous isointense	-	-	-	-
6	Hypointense, solid, heterogeneous	-	High signal	Restricted	Mild heterogeneous enhancement	-
7	Hypointense, solid-cystic	Intermediate heterogeneous signal	High signal	Restricted	Mild heterogeneous enhancement	Present
8	Hypointense, heterogeneous	Solid with small cystic areas, heterogeneous isointense	Slightly high signal	Restricted	Mild enhancement	-
9	Isointense with hemorrhage, solid-cysti	Heterogeneous isointense, edema	-	Restricted	Mild enhancement	-
10	Isointense, solid-cystic	Heterogeneous isointense	High signal, edema	Restricted	Heterogeneous enhancement	-
12	Isointense, solid	Heterogeneous isointense	High signal, edema	Restricted	Mild enhancement	-
13	Hypointense, solid with some cysts	Intermediate signal	-	Restricted	Mild heterogeneous enhancement	Present

-: Radiological finding not described.

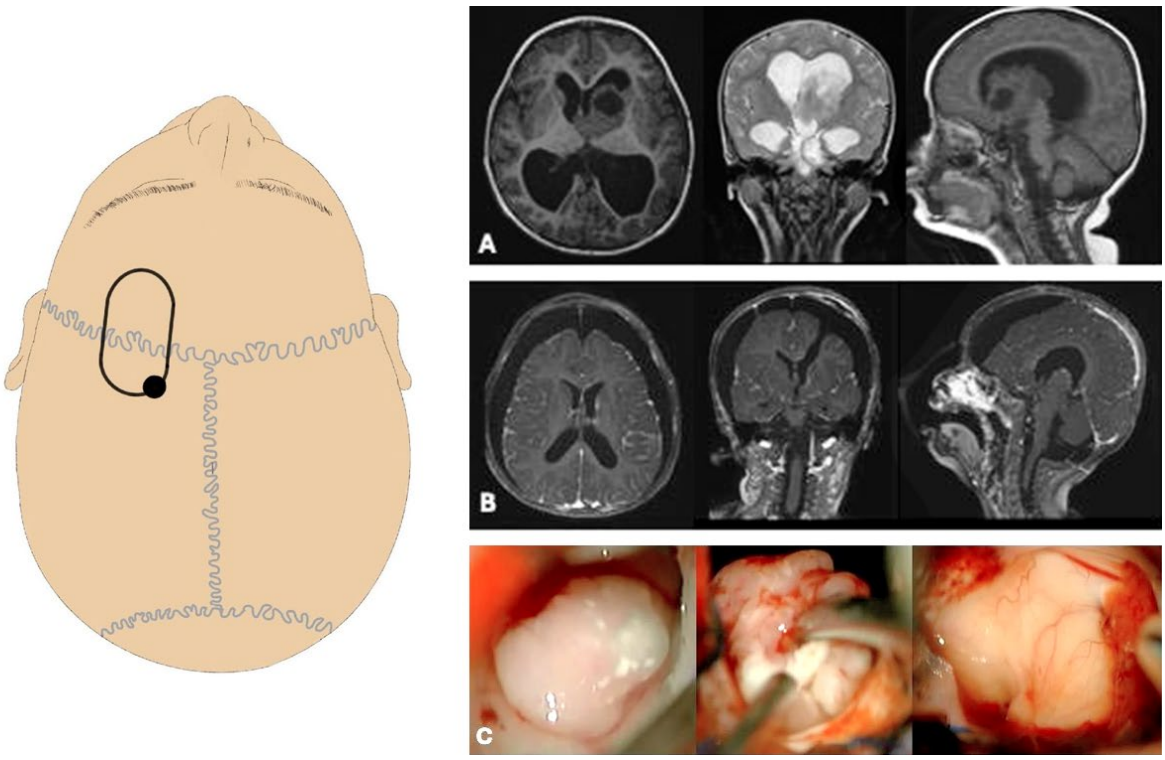

Figure 2. Left supratentorial ventricular ATRT with extension to the third ventricle, treated through a left frontal transcortical approach, whose schematic is shown in the left panel

A. Non-contrast brain MRI showing a left ventricular solid isointense lesion with a cystic component, associated with hydrocephalus and extension to the third ventricle. B. Contrast-enhanced brain MRI demonstrating total tumor resection. C. Intraoperative images showing a solid ventricular tumor, which was completely resected.

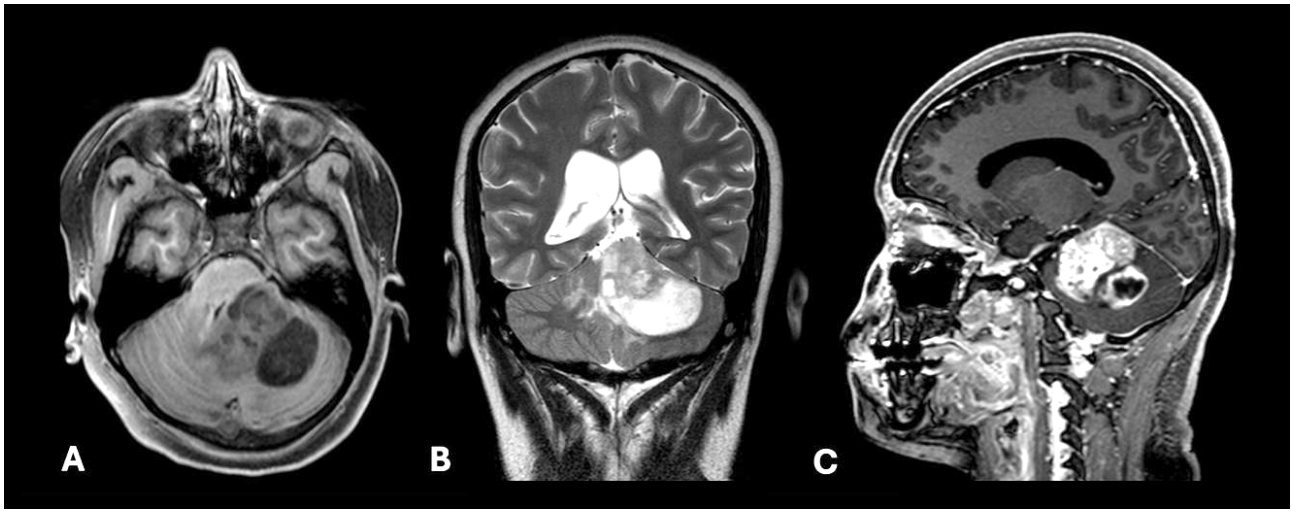

Figure 3. Brain MRI without and with contrast

A. Axial section showing a bilobulated lesion with solid and cystic components exerting mass effect in the posterior fossa. B. T2 sequence showing a heterogeneous hyperintense signal. C. Sagittal contrast-enhanced section showing a large mass occupying more than half of the posterior fossa, with heterogeneous contrast uptake and peripheral enhancement in its cystic component.

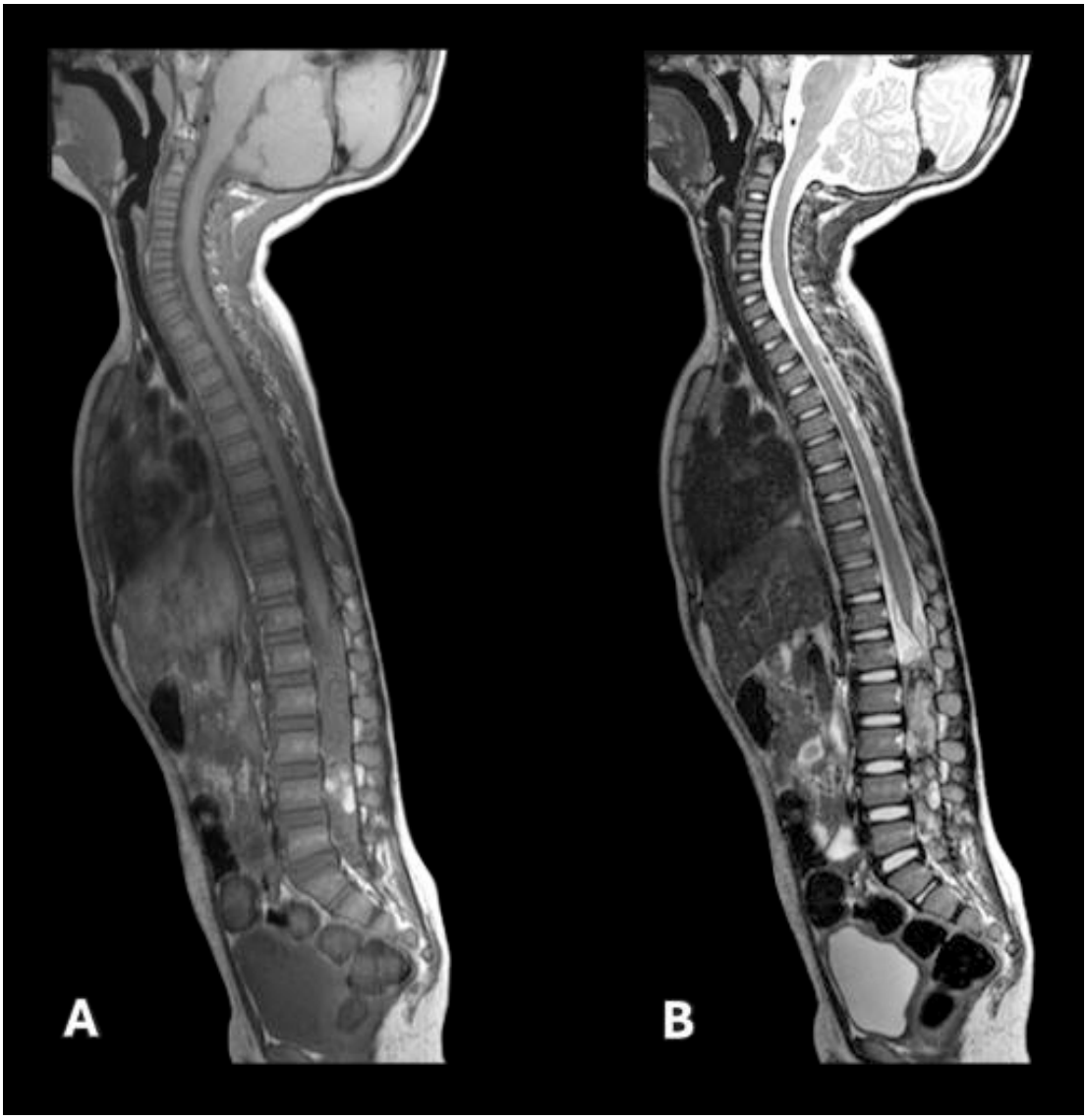

Figure 4. Whole spine MRI

A. Sagittal T1 sequence showing an isointense lesion with a hemorrhagic component at the lumbar level. B. Sagittal T2 sequence showing a heterogeneous isointense signal extending from the inferior border of the first lumbar vertebra to the second sacral vertebra.

Immunohistochemical findings are summarized in Table 5. Nine of the 14 cases (64.3%) presented rhabdoid cells, and all showed loss of nuclear INI1 expression.

Cytokeratin (CK) staining was performed in 5 patients, of whom 3 were reported as positive and 2 as negative. Synaptophysin was evaluated in all 14 cases, being positive in 13 and negative in 1. GFAP was negative in 7 cases and positive in 6, while the Ki-67 proliferation index was <50% in 6 cases, 50–70% in 5 cases, and >70% in 3 cases.

EMA staining was performed in 9 patients, with positive results in 8 and negative results in 1. Alpha-fetoprotein (AFP) was evaluated in 2 cases, both negative. CD99 staining was performed in 6 patients (4 positive and 2 negative); S-100 protein in 6 cases (3 positive and 3 negative); pancytokeratin in 4 patients (1 positive and 3 negative); and desmin in 3 cases (1 positive and 2 negative) (Table 5).

Table 5. Histopathological and immunohistochemical profile of the analyzed cases

Case	Rhabdoid cells	INI1	CK	Vimentin	Synaptophysin	GFAP	Ki-67 (%)	EMA	AFP	CD99	S100	Pancytokeratin	Desmin
1	Yes	Loss of nuclear expression	+		+	-	30						
2	Yes	Loss of nuclear expression	+		-	+	30–40	+			-		
3	Yes	Loss of nuclear expression		+	+	+	>70		-	+			
4	Yes	Loss of nuclear expression			+		40–50	+	-	+	+		
5	Yes	Loss of nuclear expression		+	+	+	20	+			+		
6	Yes	Loss of nuclear expression	-	+	+	-	60	+					
7	Yes	Loss of nuclear expression	+	+	+	+	40	+		+	+		
8	Yes	Loss of nuclear expression		+	+	-	60–70	+		+	-	-	-
9	Yes	Loss of nuclear expression			+	-	60–70	+					
10	Not reported	Loss of nuclear expression		+	+	-	30–35	-				-	
11	Not reported	Loss of nuclear expression			+	+	50–70	+				+	+
12	Not reported	Loss of nuclear expression		+	+	+	50–60					-	-
13	Not reported	Loss of nuclear expression	-	+ diffuse	+ focal	-	>70			-			
14	Not reported	Loss of nuclear expression			+ focal	-	75–80			-	-		

CK: cytokeratin; GFAP: glial fibrillary acidic protein; Ki-67: proliferation index; EMA: epithelial membrane antigen; AFP: alpha-fetoprotein; CD99: type I transmembrane protein; S100: S100 protein. Blank spaces indicate that the marker was not evaluated.

DISCUSSION

In this study, the clinical, radiological, and anatomopathological characteristics of patients diagnosed with ATRT treated at a national referral center in Lima, Peru, were described.

Regarding demographic variables, the mean age was 49 months, the median 43 months, and the range 7 to 144 months (12 years). Regarding sex, males predominated, accounting for 64.3% of cases.

The age at diagnosis reported in this study is higher than that reported in previous studies. For example, Gupta et al. (14) and Wang et al. (16) reported mean and median ages of 23 and 24 months, respectively, notably lower than those reported in this study. Similarly, in a population-based analysis conducted by Ostrom et al. (17), the median age at diagnosis was 1 year, and approximately two-thirds of cases occurred in children under 2 years of age, reinforcing that ATRT is predominantly a neoplasm of very early presentation.

Regarding sex, male predominance was also observed by Gupta et al. (14), Wang et al. (16), and Ostrom et al. (17). Although different studies consistently report a higher frequency in males, the difference observed in age could be related to social, economic, or cultural factors influencing timely access to specialized centers.

Concerning clinical manifestations, the most frequent symptoms in our population were vomiting, hydrocephalus, and headache, findings consistent with intracranial hypertension, probably secondary to tumor mass effect. Similarly, Wang et al. (16) reported vomiting as one of the most common symptoms in pediatric patients with ATRT, although in their cohort progressive limb weakness predominated. Likewise, Calandrelli et al. (18) described that the most frequent presenting symptoms were related to intracranial hypertension, including vomiting, headache, macrocephaly, and seizures, and documented the presence of acute hydrocephalus in a significant proportion of cases. These findings reinforce that, in most cases, the initial clinical presentation of ATRT is dominated by signs and symptoms of intracranial hypertension.

Regarding histopathological findings, Ud Din et al. (8) reported rhabdoid cells in 5 of 11 analyzed cases (45.45%), all of which were negative for INI1 immunoreactivity. Similarly, in our study, 9 of 14 cases (64.3%) presented rhabdoid cells, and all showed loss of nuclear INI1 expression. These findings are consistent with those reported by Al-Hussaini et al. (19), who identified rhabdoid cells as one of the most frequent cellular components of ATRT (89.5%), generally coexisting with other histological patterns. Likewise, Sigauke et al. (20) documented the complete absence of INI1 expression in all evaluated cases, reinforcing the central role of this immunohistochemical marker in diagnostic confirmation. Taken together, these data support that although the presence of rhabdoid cells is frequent, the current diagnosis of ATRT is fundamentally based on demonstrating loss of nuclear INI1 expression, as noted by Nesvick et al. (12).

ATRTs originate mainly intracranially (around 90%), with nearly 50% of cases reported in the posterior fossa. Spinal lesions remain very rare, with fewer than 50 cases reported in the English-language literature (14). In our patient group, 13 of 14 cases had intracranial location (92.9%), of which 8 were supratentorial (5 ventricular) and 5 infratentorial; only 1 case had spinal location at the lumbar level. These findings are consistent with those reported by Gupta et al. (14), who described intracranial location in approximately 90% of cases. In contrast, Wang et al. (16) reported a predominance of infratentorial tumors in their cohort (11 of 22 patients), although they also reported a low frequency of spinal involvement (2 of 22 cases). Similarly, Liu et al. (15) reported a higher proportion of tumors with infratentorial or spinal location, highlighting variability in the anatomical distribution of ATRT across different series.

When analyzing CT findings in the 10 patients evaluated, 6 showed a solid-cystic pattern, 2 a solid isodense pattern, 1 a homogeneous solid pattern, and 1 a heterogeneous solid pattern. These results differ from those reported by Kanoto et al. (21), who described a predominance of hyperdense lesions on CT in most evaluated cases (10 of 11 adult patients). In contrast, the variability observed in our pediatric cohort could be explained by intratumoral heterogeneity, including cystic components and areas of necrosis. These findings are consistent with those previously described in pediatric ATRT series, such as that reported by Ud Din et al. (8), in which lesions with cystic, necrotic, and hemorrhagic components were described, resulting in a variable tomographic appearance.

Regarding brain MRI, this was performed in only 9 of the 14 patients. On T1-weighted sequences, 5 lesions were isointense and 4 hypointense, while on T2-weighted sequences, isointense signal was observed in 6 cases and intermediate signal in 2. A frequent finding was diffusion restriction in 8 of the 9 evaluated patients, suggesting high tumor cellularity. These findings fall within the broad radiological spectrum described for ATRT. In previous pediatric series, Wang et al. (16) reported tumors that were isointense or slightly hypointense on T1, hyperintense on T2, with inhomogeneous enhancement and diffusion restriction. In contrast, Guo et al. (5) described lesions that were isointense on T1, with variable T2 signal and heterogeneous contrast enhancement. Ud Din et al. (8) and Parenrengi et al. (22), in turn, documented more complex lesions with cystic components, areas of necrosis and hemorrhage, as well as peritumoral edema, features associated with greater signal heterogeneity on MRI, in contrast to the more homogeneous appearance observed in our cohort.

Among the strengths of this study is the inclusion of patients treated at a national pediatric referral center, allowing the description of clinical and radiological characteristics of a rare neoplasm in the pediatric population within a specialized clinical setting. Additionally, the study provides original national-level information, as it constitutes the first case series of ATRT reported in Peru, with diagnosis supported by imaging and immunohistochemical studies.

However, this study has limitations. Its retrospective design and small sample size limit the generalizability of the results. Furthermore, the analyzed information is limited to data available in the institution's medical records where surgical procedures were performed.

In addition, not all patients had complete CT or MRI studies, nor a uniform immunohistochemical profile, which limits detailed comparison between cases and comprehensive tumor characterization.

Because comprehensive oncological management and postoperative follow-up of patients are performed at another specialized institution, it was not possible to include variables related to functional neurological status at admission and postoperatively, such as Glasgow, Karnofsky, or modified Rankin scales. Information on clinical outcomes such as morbidity, mortality, prognosis, or survival was also not available.

These limitations reflect the descriptive scope of the study, whose objective was to characterize the demographic, basic clinical, and histopathological aspects of the operated cases, without aiming to evaluate functional outcomes or perform analytical comparisons between groups. Therefore, the findings should be interpreted within the framework of a strictly descriptive analysis.

In conclusion, ATRTs in our cohort showed a variable clinical and radiological presentation within the spectrum described in the literature, with diagnostic confirmation based on imaging and immunohistochemical studies. This study contributes to the characterization of this rare neoplasm in the national context, recognized for its high malignancy and challenging management. Future studies should be prospective and multicenter, with longitudinal follow-up, allowing integration of clinical, histopathological, therapeutic, and survival variables to better understand the biological and clinical behavior of this entity.

Additionally, a video shows the preoperative imaging findings, the surgical approach, and the postoperative findings in one of the 14 patients included in the study, in whom complete tumor resection was achieved; the corresponding images are presented in Figures 2–4 (Video 1).

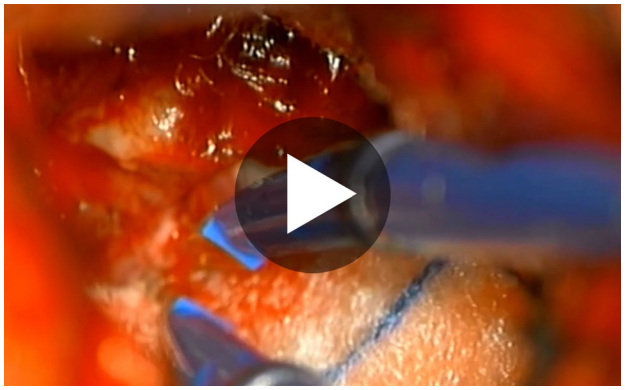

Video 1. Preoperative MRI and CT images, surgical approach, and postoperative findings in a patient with complete resection of ATRT

Author contributions

ARE: Conceptualization, Data curation, Formal analysis, Investigation, Methodology, Project administration, Supervision, Validation, Visualization, Writing – original draft, Writing – review and editing.

EDC: Conceptualization, Data curation, Investigation, Visualization, Writing – original draft, Writing – review and editing.

CCV: Investigation, Writing – original draft.

Conflicts of interest

The authors declare no relevant financial or non-financial conflicts of interest.

Funding

This study did not receive external funding.

Data availability

The data supporting the findings of this study are available upon request from the corresponding author.

REFERENCES

1. Meel MH, Guillén Navarro M, De Gooijer MC, Metselaar DS, Waranecki P, Breur M, et al. MEK/MELK inhibition and blood–brain barrier deficiencies in atypical teratoid/rhabdoid tumors. Neuro Oncol. 2020;22(1):58-69. doi: 10.1093/neuonc/noz151
2. Richardson EA, Ho B, Huang A. Atypical Teratoid Rhabdoid Tumour: From Tumours to Therapies. J Korean Neurosurg Soc. 2018;61(3):302-11. doi: 10.3340/jkns.2018.0061
3. Nesvick CL, Lafay-Cousin L, Raghunathan A, Bouffet E, Huang AA, Daniels DJ. Atypical teratoid rhabdoid tumor: molecular insights and translation to novel therapeutics. J Neurooncol. 2020;150(1):47-56. doi: 10.1007/s11060-020-03639-w
4. Gastberger K, Fincke VE, Mucha M, Siebert R, Hasselblatt M, Frühwald MC. Current Molecular and Clinical Landscape of ATRT - The Link to Future Therapies. Cancer Manag Res. 2023;15:1369-93. doi: 10.2147/CMAR.S379451
5. Guo G, Zhuang J, Zhang K, Zhou Z, Wang Y, Zhang Z. Atypical Teratoid/Rhabdoid Tumor of the Central Nervous System in Children: Case Reports and Literature Review. Front Surg. 2022;9:864518. doi: 10.3389/fsurg.2022.864518
6. Louis DN, Perry A, Wesseling P, Brat DJ, Cree IA, Figarella-Branger D, et al. The 2021 WHO Classification of Tumors of the Central Nervous System: a summary. Neuro Oncol. 2021;23(8):1231-51. doi: 10.1093/neuonc/noab106
7. Goulart Corrêa D, Rachid De Souza S, Ventura N, Camacho AH, Chimelli L, Gasparetto EL. Suprasellar atypical teratoid/rhabdoid tumor. J Neuroradiol. 2017;44(4):288-90. doi: 10.1016/j.neurad.2017.03.002
8. Ud Din N, Barakzai A, Memon A, Hasan S, Ahmad Z. Atypical Teratoid/Rhabdoid Tumor of Brain: a Clinicopathologic Study of Eleven Patients and Review of Literature. Asian Pac J Cancer Prev. 2017;18(4):949-54. doi: 10.22034/APJCP.2017.18.4.949
9. Wu HW, Wu CH, Lin SC, Wu CC, Chen HH, Chen YW, et al. MRI features of pediatric atypical teratoid rhabdoid tumors and medulloblastomas of the posterior fossa. Cancer Med. 2023;12(9):10449-61. doi: 10.1002/cam4.5780
10. Phuttharak W, Wannasarnmetha M, Wara-asawapati S, Yuthawong S. Diffusion MRI in Evaluation of Pediatric Posterior Fossa Tumors. Asian Pac J Cancer Prev. 2021;22(4):1129-36. doi: 10.31557/APJCP.2021.22.4.1129
11. Martínez Tamborini N, Báez A, Casas Parera I, Halfon MJ, Báez M, Blumenkrantz Y, et al. Tumores gliales del sistema nervioso: planificación y porcentaje de resección. Neurol Argent. 2013;5(2):129-32. doi: 10.1016/j.neuarg.2013.02.004
12. Nesvick CL, Nageswara Rao AA, Raghunathan A, Biegel JA, Daniels DJ. Case-based review: atypical teratoid/rhabdoid tumor. Neurooncol Pract. 2019;6(3):163-78. doi: 10.1093/nop/npy037
13. Park M, Han JW, Hahn SM, Lee JA, Kim JY, Shin SH, et al. Atypical Teratoid/Rhabdoid Tumor of the Central Nervous System in Children under the Age of 3 Years. Cancer Res Treat. 2021;53(2):378-88. doi: 10.4143/crt.2020.756
14. Gupta NK, Godbole N, Sanmugananthan P, Gunda S, Kasula V, Baggett M, et al. Management of Atypical Teratoid/Rhabdoid Tumors in the Pediatric Population: A Systematic Review and Meta-Analysis. World Neurosurg. 2024;181:e504-15. doi: 10.1016/j.wneu.2023.10.089
15. Liu YL, Tsai ML, Chen CI, Yar N, Tsai CW, Lee HL, et al. Atypical Teratoid/Rhabdoid Tumor in Taiwan: A Nationwide, Population-Based Study. Cancers. 2022;14(3):668. doi: 10.3390/cancers14030668

16. Wang RF, Guan WB, Yan Y, Jiang B, Ma J, Jiang MW, et al. Atypical teratoid/rhabdoid tumours: clinicopathological characteristics, prognostic factors and outcomes of 22 children from 2010 to 2015 in China. Pathology (Phila). 2016;48(6):555-63. doi: 10.1016/j.pathol.2016.05.010
17. Ostrom QT, Chen Y, de Blank PM, Ondracek A, Farah P, Gittleman H, et al. The descriptive epidemiology of atypical teratoid/rhabdoid tumors in the United States, 2001-2010. Neuro Oncol. 2014;16(10):1392-9. doi: 10.1093/neuonc/nou090
18. Calandrelli R, Massimi L, Pilato F, Verdolotti T, Ruggiero A, Attinà G, et al. Atypical Teratoid Rhabdoid Tumor: Proposal of a Diagnostic Pathway Based on Clinical Features and Neuroimaging Findings. Diagnostics (Basel). 2023;13(3):475. doi: 10.3390/diagnostics13030475
19. Al-Hussaini M, Dissi N, Souki C, Amayiri N. Atypical teratoid/rhabdoid tumor, an immunohistochemical study of potential diagnostic and prognostic markers. Neuropathology. 2016;36(1):17-26. doi: 10.1111/neup.12231
20. Sigauke E, Rakheja D, Maddox DL, Hladik CL, White CL, Timmons CF, et al. Absence of expression of SMARCB1/INI1 in malignant rhabdoid tumors of the central nervous system, kidneys and soft tissue: an immunohistochemical study with implications for diagnosis. Mod Pathol. 2006;19(5):717-25. doi: 10.1038/modpathol.3800581
21. Kanoto M, Toyoguchi Y, Hosoya T, Kuchiki M, Sugai Y. Radiological Image Features of the Atypical Teratoid/Rhabdoid Tumor in Adults: A Systematic Review. Clin Neuroradiol. 2015;25(1):55-60. doi: 10.1007/s00062-013-0282-2
22. Parenrengi MA, Permana GI, Suryaningtyas W, Fauziah D. The aggressive progression of primary intracranial atypical teratoid/rhabdoid tumor after surgical resection: A case report. Int J Surg Case Rep. 2022;91:106790. doi: 10.1016/j.ijscr.2022.106790